Solid State Communications 245 (2016) 11–14

Contents lists available at ScienceDirect

Solid State Communications

journal homepage: www.elsevier.com/locate/ssc

Communication

# Superconductivity in $CeOBiS_2$ with cerium valence fluctuation

Masanori Nagao [a,*], Akira Miura [b], Ikuo Ueta [a], Satoshi Watauchi [a], Isao Tanaka [a]

[a] University of Yamanashi, 7-32 Miyamae, Kofu, Yamanashi 400-8511, Japan
[b] Hokkaido University, Kita13 Nishi8, Kita-ku, Sapporo, Hokkaido 060-8628, Japan

ARTICLE INFO

*Article history:*
Received 25 April 2016
Received in revised form
14 July 2016
Accepted 15 July 2016
Available online 17 July 2016

*Keywords:*
A. $BiS_2$-based superconductor
D. Superconductivity
E. Adiabatic demagnetization refrigerator
Valence fluctuation

ABSTRACT

Resistivities of single-crystalline as well as poly-crystalline samples of $CeOBiS_2$ without fluorine doping were measured at temperatures down to 0.13 K, and were compared with those of poly-crystalline $LaOBiS_2$ and $PrOBiS_2$. Both poly-crystalline and single-crystalline $CeOBiS_2$ exhibited zero resistivity below 1.2 K while poly-crystalline $LaOBiS_2$ and $PrOBiS_2$ did not show zero resistivity down to 0.13 K. Superconducting transition temperature of $CeOBiS_2$ was reduced by increasing the applied current density. The superconductivity of $CeOBiS_2$ without chemical doping is likely triggered by the carriers induced by the valence fluctuation between $Ce^{3+}$ and $Ce^{4+}$.



## 1. Introduction

Chemical doping of semiconductors is a method used to induce superconductivity in them. The superconductivity of diamond [1,2], Si [3], and SiC [4–6] is induced by introducing carriers through chemical doping. $R(O,F)BiS_2$ ($R$=La, Ce, Pr, Nd, Yb) [7–11] are layered semiconductors with a band gap of around 1 eV [12], and superconductivity is induced in them through electron carrier doping by substituting oxygen (O) with fluorine (F). This doping induces electron carriers into the $BiS_2$ superconducting layer. Recently, it was discovered that the fluctuation of Eu valence between $Eu^{2+}$ and $Eu^{3+}$ induces carriers and produces superconductivity in $EuFBiS_2$ and $Eu_3Bi_2S_4F_4$ without chemical doping [13,14]. Thus, Eu-based compounds are examples in which superconductivity is induced by the fluctuation of valence. As suggested in Refs. [15,16], for $R$=Ce, the Ce valence in $CeOBiS_2$ also fluctuates between $Ce^{3+}$ and $Ce^{4+}$. However, its zero resistivity has not been reported at a temperature down to 1.8 K in F-free $CeOBiS_2$. This motivated us to examine superconductivity in non-chemically doped $CeOBiS_2$ to investigate whether a valence fluctuation can induce superconductivity in general. In this paper, we measured the temperature dependence of electrical resistivity for chemically non-doped $ROBiS_2$ ($R$=La, Ce, Pr) poly crystals and $CeOBiS_2$ single crystals down to 0.13 K using an adiabatic demagnetization refrigerator (ADR). In contrast to $LaOBiS_2$ and $PrOBiS_2$, only $CeOBiS_2$ showed superconducting transition below 1.2 K, indicating that the valence fluctuation of Ce induces superconductivity.

## 2. Experimental

Poly-crystalline samples of $ROBiS_2$ ($R$=La, Ce, Pr) were synthesized by a solid state reaction in a vacuumed quartz tube using $R_2S_3$ (99.9 wt%), $Bi_2S_3$ (99.9 wt%), and $Bi_2O_3$ (99.9 wt%) as raw materials. The raw materials were mixed in a nominal composition of $ROBiS_2$ using a mortar, and sealed into a quartz tube in vacuum (~10 Pa). Then, the sample was heated at 700 °C for 10 h. The calcined mixture was ground to homogenize it and pressed into a pellet of 10 mm diameter and about 1–2 mm thickness, and then sealed in a quartz tube under vacuum (~10 Pa). This pellet in the quartz tube was heated at 700 °C for 20 h, and then furnace-cooled to room temperature. The quartz tube was opened in air. Poly-crystalline samples of $ROBiS_2$ were obtained as products.

Single crystals of $CeOBiS_2$ were grown by the CsCl flux method in a vacuumed quartz tube using $Ce_2S_3$ (99.9 wt%), $Bi_2S_3$ (99.9 wt%), $Bi_2O_3$ (99.9 wt%), and CsCl (99.8 wt%) as raw materials [17–20]. The raw materials were weighed to obtain the nominal composition of $CeOBiS_2$. A mixture of these raw materials (0.8 g) and CsCl flux (5.0 g) was combined using a mortar, and then sealed in a quartz tube under vacuum (~10 Pa). This mixed powder in the quartz tube was heated at 950 °C for 10 h, cooled slowly to 650 °C at a rate of 1 °C/h, and then furnace-cooled to room temperature. The quartz tube was opened in air, and the flux was dissolved in the quartz tube using distilled water. The product obtained was filtered and washed with distilled water.

The crystal structures of the poly-crystalline and single-crystalline products were evaluated by X-ray diffraction (XRD) analysis using CuK$\alpha$ radiation. The resistivity–temperature ($\rho$–$T$) characteristics of these poly-crystalline and single-crystalline samples were measured by the standard four-probe method at a constant

* Correspondence to: Postal address: University of Yamanashi, Center for Crystal Science and Technology, Miyamae 7-32, Kofu 400-8511, Japan.
*E-mail address:* mnagao@yamanashi.ac.jp (M. Nagao).

http://dx.doi.org/10.1016/j.ssc.2016.07.017
0038-1098/

current density ($J$) using an ADR option for quantum design physical property measurement system (PPMS). The magnetic field applied for operating the ADR was 3 T at 1.9 K; subsequently, it was removed. Consequently, the temperature of sample decreased to around 0.13 K. The measurement of $\rho$–$T$ characteristics was started at the lowest temperature (around 0.13 K), which was spontaneously increased to around 15 K. The $\rho$–$T$ characteristics were measured while the temperature was increased. The dependence of applied current density on the $\rho$–$T$ characteristics was also observed. The superconducting transition temperature ($T_c$) was estimated from the $\rho$–$T$ characteristics. The transition temperature corresponding to the onset of superconductivity ($T_c^{onset}$) is defined as the temperature at which deviation from linear behavior is observed in the normal conducting state in the $\rho$–$T$ characteristics. The zero resistivity ($T_c^{zero}$) is determined as the temperature at which resistivity is below 5 μΩ cm. $\rho$–$T$ characteristics under a magnetic field ($H$) range of 0–0.3 T parallel to the $ab$-plane and the $c$-axis of $CeOBiS_2$ single crystal were measured without ADR option in the temperature range of 2.0–5.0 K.

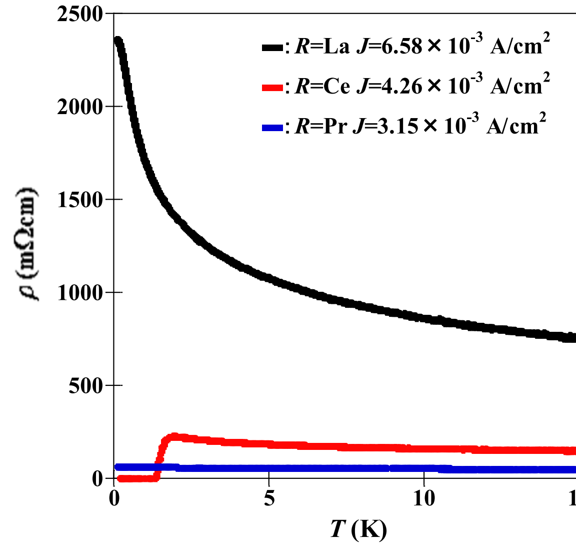


**Fig. 2.** (Color online) $\rho$–$T$ characteristics of $R$OBiS$_2$ poly-crystalline samples at 0.13–15 K using ADR option.

## 3. Results and discussion

Fig. 1 shows the XRD patterns of $R$OBiS$_2$ poly-crystalline samples where (a) $R$=La, (b) $R$=Ce, and (c) $R$=Pr. The major diffraction peaks of the obtained poly-crystalline samples were indexed as $R$OBiS$_2$ phases. Fig. 2 shows the $\rho$–$T$ characteristics of $R$OBiS$_2$ poly-crystalline samples in the temperature range of 0.13–15 K. $LaOBiS_2$ and $PrOBiS_2$ poly-crystalline samples did not exhibit zero resistivity down to around 0.13 K. In contrast, for $R$=Ce, the resistivity drops in the range 1.3–1.9 K; the $T_c^{onset}$ and $T_c^{zero}$ were estimated to be 1.9 K and 1.3 K, respectively. The transport properties of the $R$OBiS$_2$ poly-crystalline samples exhibited semiconducting behavior. $LaOBiS_2$ showed a significantly higher resistivity compared to $CeOBiS_2$ and $PrOBiS_2$. The resistivity of $PrOBiS_2$ was lower than that of $CeOBiS_2$ at the normal state. However, superconducting transition was not observed in $PrOBiS_2$ down to 0.13 K.

Fig. 3 shows the XRD pattern of a well-developed plane of $CeOBiS_2$ single crystal. The presence of only 00$l$ diffraction peaks of

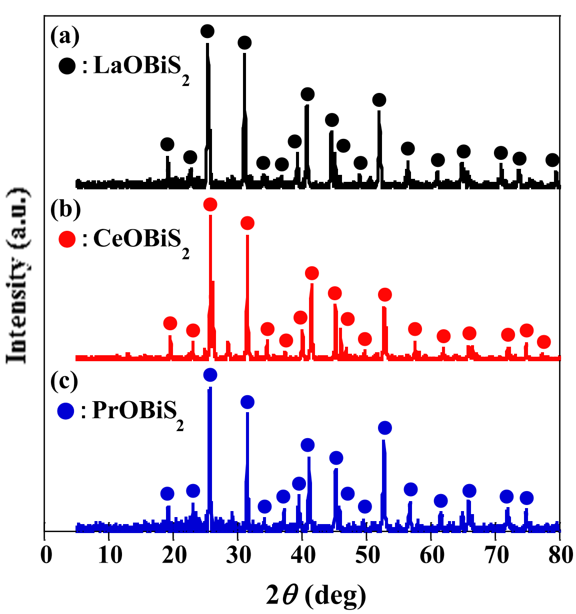


**Fig. 1.** (Color online) XRD pattern of $R$OBiS$_2$ poly-crystalline samples where (a) $R$=La, (b) $R$=Ce and (c) $R$=Pr.

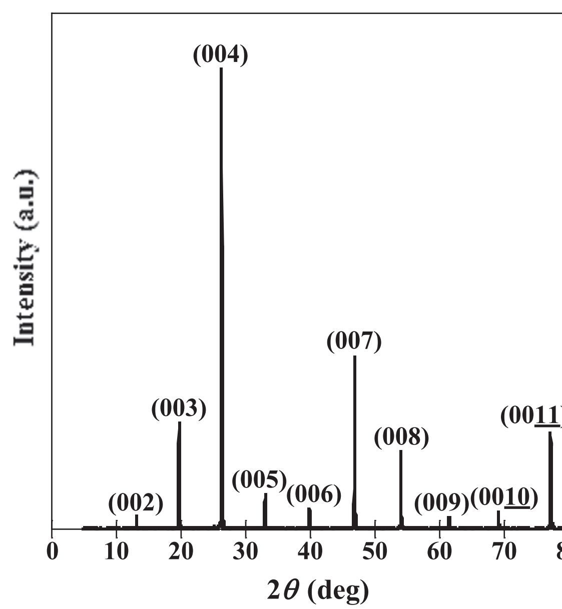


**Fig. 3.** XRD pattern of well-developed plane of $CeOBiS_2$ single crystal.

the $CeOBiS_2$ structure indicates that the $ab$-plane is well developed. Four terminals for the $\rho$–$T$ characteristics measurement were fabricated on the well-developed plane using silver paste. In consequence, the applied current was along the $ab$-plane. The $\rho$–$T$ characteristics of the $CeOBiS_2$ single crystal sample were measured in the temperature range of 0.13–15 K. Fig. 4 shows the applied current density dependence of $\rho$–$T$ characteristics for a $CeOBiS_2$ single crystal. Superconducting transition was observed in the $CeOBiS_2$ single crystal, and the superconducting transition temperature was reduced by increasing the applied current density ($J$). The $T_c^{zero}$ was not observed down to 0.13 K, when $J$ was more than 6.33 A/cm$^2$. For $J$=1.05 A/cm$^2$, the $T_c^{onset}$ and $T_c^{zero}$ were estimated to be 3.1 K and 1.2 K, respectively. Similar $T_c^{zero}$ found in poly-crystalline and single-crystalline samples suggests that $CeOBiS_2$ without intentional doping displays superconductivity below 1.2 K. Nonetheless, there are minor differences in transition temperatures between poly-crystalline and single-crystalline samples. The $T_c^{zero}$ of single-crystal sample (1.2 K) was slightly